Cell

Coronin 1B Coordinates Arp2/3 Complex and Cofilin Activities at the Leading Edge

Liang Cai,[1] Thomas W. Marshall,[1] Andrea C. Uetrecht,[1] Dorothy A. Schafer,[2] and James E. Bear[1,*]
[1] Lineberger Comprehensive Cancer Center and Department of Cell and Developmental Biology, School of Medicine, University of North Carolina at Chapel Hill, Chapel Hill, NC 27599, USA
[2] Departments of Biology and Cell Biology, University of Virginia, Charlottesville, VA 22904, USA
*Correspondence: jbear@email.unc.edu
DOI 10.1016/j.cell.2007.01.031

SUMMARY

Actin filament formation and turnover within the treadmilling actin filament array at the leading edge of migrating cells are interdependent and coupled, but the mechanisms coordinating these two activities are not understood. We report that Coronin 1B interacts simultaneously with Arp2/3 complex and Slingshot (SSH1L) phosphatase, two regulators of actin filament formation and turnover, respectively. Coronin 1B inhibits filament nucleation by Arp2/3 complex and this inhibition is attenuated by phosphorylation of Coronin 1B at Serine 2, a site targeted by SSH1L. Coronin 1B also directs SSH1L to lamellipodia where SSH1L likely regulates Cofilin activity via dephosphorylation. Accordingly, depleting Coronin 1B increases phospho-Cofilin levels, and alters lamellipodial dynamics and actin filament architecture at the leading edge. We conclude that Coronin 1B's coordination of filament formation by Arp2/3 complex and filament turnover by Cofilin is required for effective lamellipodial protrusion and cell migration.

INTRODUCTION

Coronins are highly-conserved F-actin binding proteins (Uetrecht and Bear, 2006). Functional studies in *Dicytostelium* amoeba, fibroblasts and thymocytes indicate that Coronins play an important role in lamellipodial protrusion, whole-cell motility and chemotaxis (Cai et al., 2005; de Hostos et al., 1993; Foger et al., 2006; Mishima and Nishida, 1999), but the mechanism(s) by which Coronins influence motility are unknown. In yeast, one mechanism may be through inhibition of Arp2/3 complex (Humphries et al., 2002; Rodal et al., 2005), but the effects of mammalian Coronins on actin nucleation activity by Arp 2/3 complex are unknown. Mammalian Coronin 1B is ubiquitously expressed and localizes to the leading edge of migrating fibroblasts (Cai et al., 2005). The interactions of Coronin 1B or Coronin 1A with Arp2/3 complex are regulated by phosphorylation of Serine 2 via PKC, where phosphorylation of Ser2 reduced the interaction with Arp2/3 and diminished cell motility (Cai et al., 2005; Foger et al., 2006).

ADF/Cofilin proteins (hereafter referred to as Cofilin) control actin filament turnover at the leading edge and at other cellular locations (Bamburg, 1999). Mechanistically, Cofilin severs and potentially enhances depolymerization of filaments by cooperatively binding along the sides of actin filaments and inducing conformational changes in filament structure (Bamburg et al., 1999). In vivo, Cofilin regulates the dynamics of actin-based structures such as stress fibers, dendritic spines and lamellipodia (Dawe et al., 2003; Hotulainen et al., 2005; Zhou et al., 2004). The activity of Cofilin is regulated in a variety of ways including phosphorylation, PIP_2 binding, intracellular pH changes and interactions with binding partners such as AIP1 (Bamburg, 1999).

Phosphorylation of Cofilin-serine 3 by LIM Kinase or TESK leads to decreased F-actin binding and inactivation of Cofilin (Stanyon and Bernard, 1999). Dephosphorylation of Serine 3 on Cofilin enhances F-actin binding and activates its severing/depolymerization activity (Agnew et al., 1995). Two classes of phosphatases act on Cofilin - the Slingshots and Chronophin (Huang et al., 2006). Slingshot is a family of atypical Serine/Threonine protein phosphatases that in mammals includes Slingshot-1, -2 and -3; Slingshot-1 and -2 exist as long and short isoforms (Niwa et al., 2002; Ohta et al., 2003). The long isoform of Slingshot-1 (SSH1L) functions during chemotaxis of hematopoeitic cells (Nishita et al., 2005). Regulation of SSH1L activity may occur via phosphorylation of serine residues in its C terminus and binding of inhibitory 14-3-3 proteins (Nagata-Ohashi et al., 2004). In addition, SSH1L activity is greatly enhanced by its interaction with F-actin (Nagata-Ohashi et al., 2004; Soosairajah et al., 2005). The other known Cofilin phosphatase, Chronophin, is a HAD-type serine phosphatase that plays an important role in cytokinesis (Gohla et al., 2005).

Considerable evidence suggests that the activities of Arp2/3 complex and Cofilin are coordinately regulated at the leading edge of motile cells. Studies using correlative microscopy (Svitkina and Borisy, 1999) suggest an array treadmilling model for actin assembly and turnover within lamellipodia in which Arp2/3-dependent filament nucleation at the front of the lamellipodia was balanced by Cofilin-dependent depolymerization of filaments at the rear. Arp2/3 complex and Cofilin also work together to promote lamellipodial protrusion in quiescent adenocarcinoma cells stimulated with growth factors, albeit via a different mechanism (DesMarais et al., 2005). MTLn3 cells stimulated with EGF initiate protrusion when Cofilin severs filaments creating new barbed ends that are preferred sites for Arp2/3-dependent filament nucleation (Ichetovkin et al., 2002). Together, filament severing and filament nucleation synergize to produce a burst of new barbed ends at the leading edge that support lamellipodial protrusion (DesMarais et al., 2004). Finally, studies using quantitative fluorescent speckle microscopy in epithelial cells suggest that Arp2/3 complex and Cofilin activities within lamellipodia may be coupled (Ponti et al., 2005), but very little is known about how this occurs. In this work, we describe a molecular connection between the Arp2/3 complex and Cofilin activities at the leading edge of motile cells that involves Coronin 1B.

RESULTS

Depletion of Coronin 1B Reduces Whole-Cell Motility and Modulates Lamellipodial Dynamics

To test the role of Coronin 1B in motility, we depleted Coronin 1B in Rat2 cells and monitored the effects on whole-cell migration and lamellipodial dynamics. An shRNA that selectively targets mouse and rat, but not human, Coronin 1B (Figures 1A and 1B) decreased the level of Coronin 1B in mouse or rat cells (Figures 1C and 4J) (Rubinson et al., 2003). Depletion of Coronin 1B leads to ~33% decrease in cell speed relative to uninfected cells, cells infected with a control shRNA (NS) or cells expressing the Coronin 1B shRNA and human Coronin 1B-GFP that is refractory to the shRNA (Figure 1D). Since the decreased rate of cell motility was rescued by expressing human Coronin 1B-GFP, this effect is specifically due to loss of Coronin 1B and not off-target silencing. Thus, Coronin 1B is required for normal whole-cell motility.

Since Coronin 1B is concentrated at the leading edge (Figure S1 in the Supplemental Data available with this article online), we reasoned that the effects of Coronin 1B depletion on whole-cell motility might arise from defects in lamellipodial dynamics. We used kymography to quantify the effects of Coronin 1B depletion on lamellipodial dynamics (Figure 1E). Three parameters of lamellipodial behavior were analyzed: protrusion rate, protrusion persistence and protrusion distance (Hinz et al., 1999). Depletion of Coronin 1B increased the protrusion rate and decreased the protrusion persistence and the distance protruded (Figure 1F). Thus, Coronin 1B modulates lamellipodial dynamics, but is not absolutely required for protrusions to form.

Depletion of Coronin 1B Slows Retrograde Actin Flow, Influences Barbed End Distribution and Density, and Influences Actin Architecture at the Leading Edge

The assembly and disassembly of actin filament networks underlie the dynamic behavior of lamellipodia. Since Coronin 1B depletion affects lamellipodia and Coronins bind F-actin, we tested if Coronin 1B depletion affects actin dynamics at the leading edge. The network of actin filaments assembling at the cell margin moves rearwards toward the cell body via retrograde flow. Using kymography of cells expressing GFP-actin to visualize actin, the rate of retrograde actin flow in Coronin 1B-depleted cells was reduced to ~50% the rate in control cells (Figures 2A and 2B), supporting the idea that Coronin 1B modulates the dynamics of the actin network at the leading edge.

A zone of rapidly growing filament barbed ends is a hallmark of the actin network at the leading edge (Condeelis et al., 1988). To measure the distribution and density of barbed ends in Coronin 1B depleted cells, we used an established assay to monitor barbed ends *in situ* (Symons and Mitchison, 1991). Depletion of Coronin 1B leads to a striking narrowing of the zone of barbed ends near the cell edge compared to control cells (Figures 2C and 2D). In addition to altering the spatial distribution of barbed ends, Coronin 1B depletion increased the density of barbed ends relative to total F-actin (Figure 2E). Thus, Coronin 1B inhibits the generation of barbed ends at the leading edge and alters their spatial distribution.

To examine the underlying actin filament architecture at the leading edge of Coronin 1B depleted cells, we used platinum replica electron microscopy. Rat2 cells have a robust and uniform dendritic network of actin filaments at the leading edge that is approximately 2μm wide (Figure 2F). Cells depleted of Coronin 1B have an abnormal actin network characterized by densely branched filaments at the cell margin and a relative paucity of actin filaments at the rear of the lamellipodium (Figure 2F). These changes in the organization of actin filaments are not observed in cells expressing a control shRNA or in Coronin 1B-depleted cells rescued with human Coronin 1B-GFP (Figure S3). Thus, Coronin 1B appears to plays a role in coordinating assembly of actin filaments at the cell edge and disassembly of actin filaments at the rear of the lamellipodium.

Coronin 1B Inhibits Arp2/3 Complex Activity in a Phosphorylation-Dependent Manner

Yeast Coronin inhibits actin filament nucleation by Arp2/3 complex in vitro (Humphries et al., 2002). To determine if human Coronin 1B inhibits Arp2/3 complex nucleation activity, we added recombinant Coronin 1B to pyrenyl actin polymerization reactions. Coronin 1B had no effect on the rates of spontaneous actin assembly or of assembly

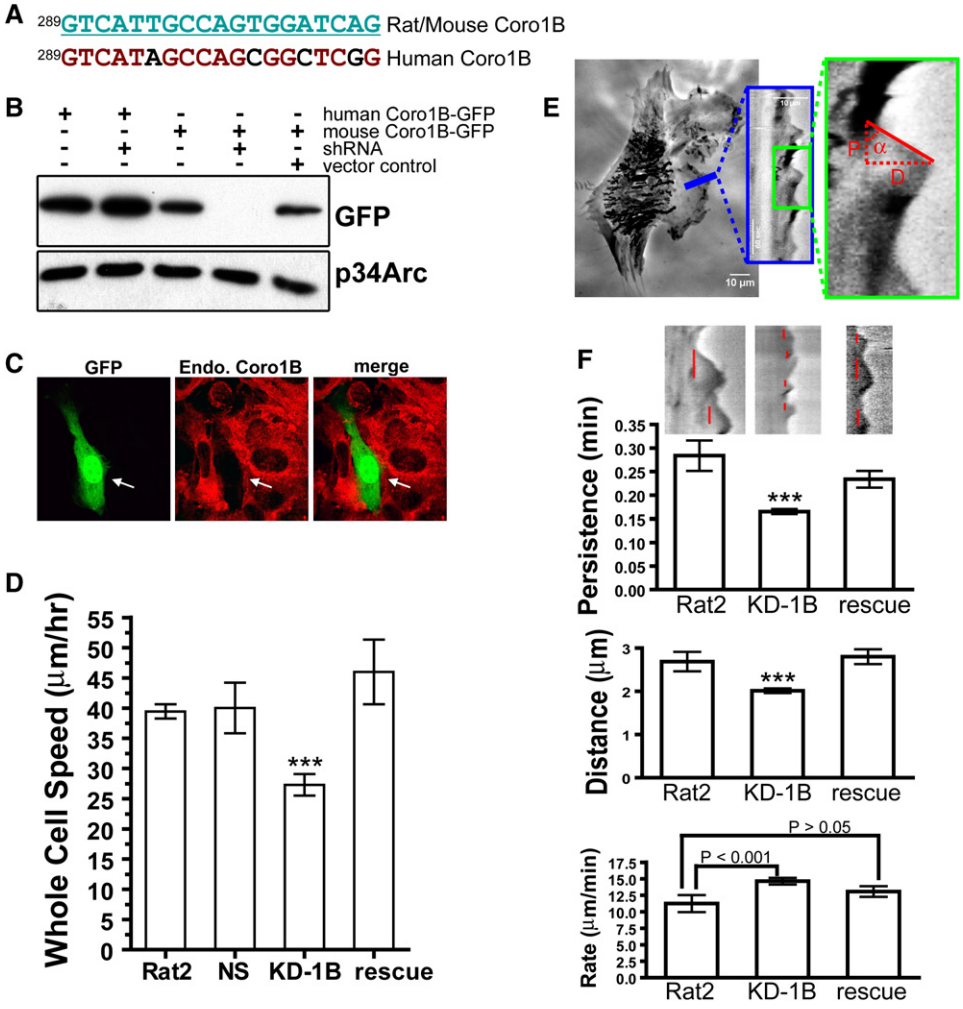

Figure 1. Depletion of Coronin 1B Slows Whole-Cell Migration and Alters Lamellipodial Dynamics

(A) Target sequence of an shRNA designed to deplete mouse or rat, but not human, Coronin 1B.

(B) HEK293 cells were cotransfected with the Coronin 1B shRNA and GFP-tagged human or mouse Coronin 1B. Lysates were blotted with anti-GFP to verify the efficiency and species specificity of knockdown. p34Arc protein was detected as a loading control.

(C) NIH3T3 cells were transfected with Coronin 1B shRNA (indicated by GFP) for 72 hr, and immunostained for Coronin 1B (red) to verify endogenous gene knockdown.

(D) Mean cell speeds of Rat2 cells expressing Coronin 1B shRNA (KD-1B, without or with (rescue) expression of GFP-tagged human Coronin 1B) or control shRNA (NS). Newman-Keuls multiple comparison test was used after one-way ANOVA to generate the p values ($p < 0.001$); error bars represent 95% CI.

(E) Method for kymography analysis. Minimal intensity projection of a 300-frame 1 s interval movie is presented on the right. Pixel intensities along a 1-pixel wide line (blue) were used to generate the kymograph presented in the blue box; a magnified region (outlined in green) is displayed on the right. Red dashed lines indicate the parameters for one protrusion. Abbreviations are as follows: D, protrusion distance; P, protrusion persistence; and $\tan\alpha$, protrusion rate.

(F) Protrusion parameters of Rat2 cells expressing the Coronin 1B shRNA without or with coexpression of human Coronin 1B (rescue). Sample kymographs are shown above each bar; red lines indicate persistence time for each protrusion. Mean value is presented; error bars represent 95% CI. Newman-Keuls multiple comparison test was used after one-way ANOVA to generate the p values ($p < 0.001$ compared to Rat2).

nucleated from Spectrin-F-actin seeds (Figure S6). However, in reactions containing Coronin 1B and GST-VCA-activated Arp2/3 complex, the rate of actin polymerization was reduced (Figures 3A and 3B). To determine if phosphorylation at Ser2 regulates Coronin 1B's inhibition of Arp2/3 complex, we compared wild-type Coronin 1B (WT), phosphorylated Coronin 1B (p-WT) and a phosphomimetic S2D mutant of Coronin 1B. In contrast to WT Coronin 1B, phosphorylated Coronin 1B (p-WT) and the S2D mutant Coronin 1B weakly inhibit Arp2/3 complex nucleation activity at all doses tested (Figures 3B and S7). Furthermore, purified Arp2/3 complex bound directly to wild-type Coronin 1B, but did not bind to the phosphomimetic S2D Coronin 1B mutant (Figure 3C). Thus, Coronin

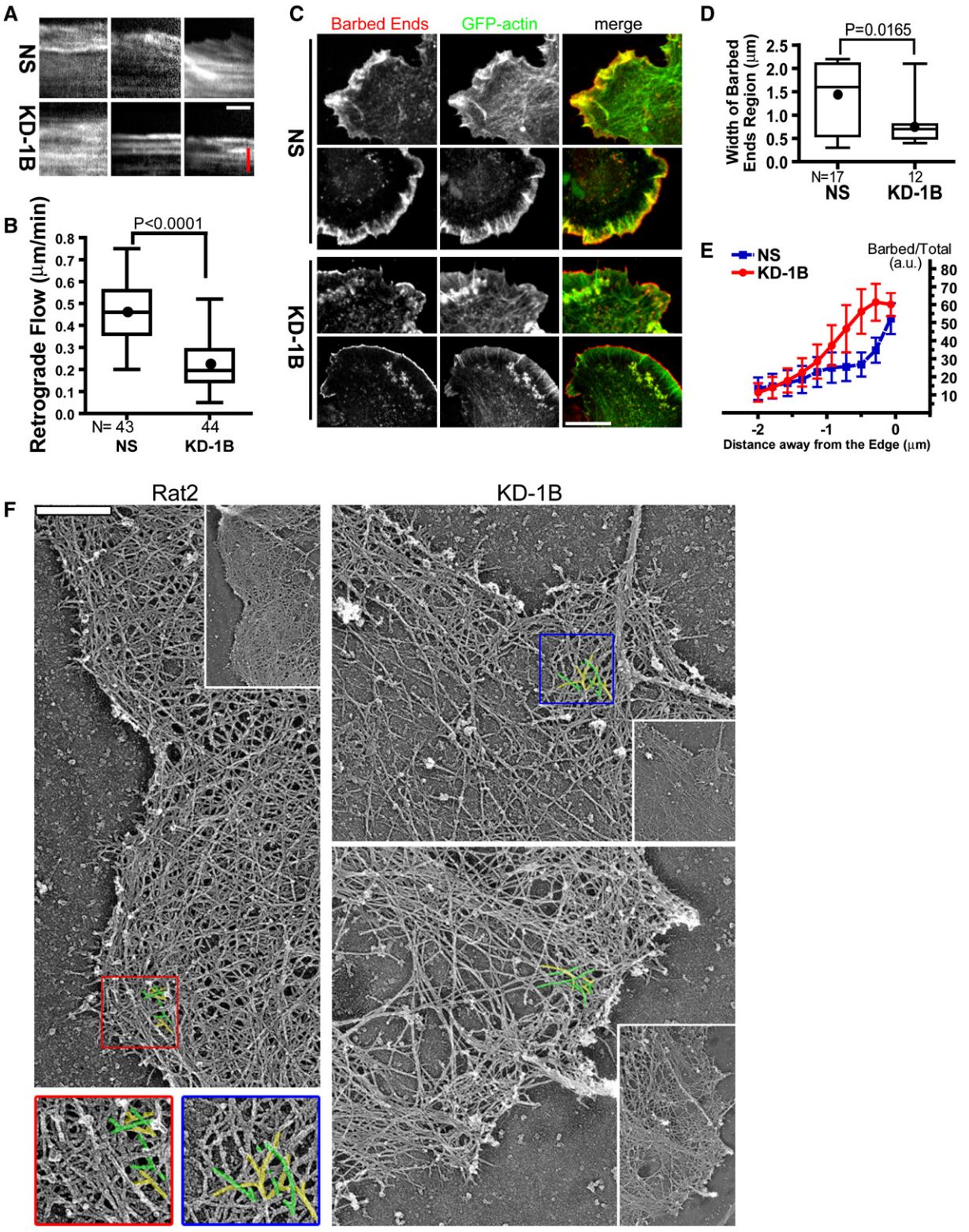

Figure 2. Depletion of Coronin 1B Slows Retrograde Actin Flow, Influences Barbed End Distribution and Filament Architecture at the Leading Edge

(A) Representative kymographs showing retrograde actin flow are shown for Rat2 cells coexpressing either Coronin 1B (KD-1B) or control (NS) shRNA and GFP-actin. Red bar represents 1.14 μm; white bar represents 30 s.

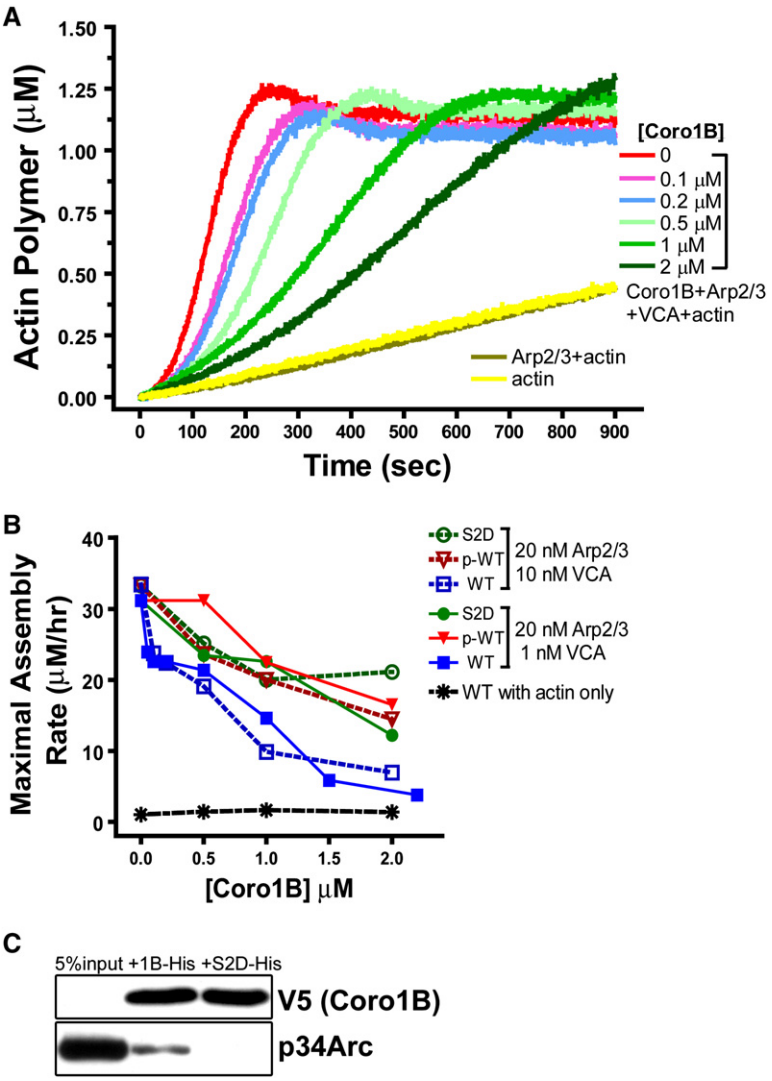

Figure 3. Coronin 1B Inhibits Actin Nucleation by Arp2/3 Complex In Vitro

(A) Actin polymer concentrations versus time in reactions containing 1.5 μM actin (5% pyrene labeled), 20 nM Arp2/3 complex, 10 nM GST-VCA, and Coronin 1B as indicated. The curves labeled actin (yellow) and Arp2/3+actin (tan) contained neither Coronin 1B nor GST-VCA.

(B) The maximal rates of actin polymerization at varying Coronin 1B concentrations. Abbreviations are as follows: WT, wild-type Coronin 1B (no detectable phosphorylation); p-WT, wild-type Coronin 1B purified from PMA-stimulated cells (~75% phosphorylated); S2D, a mutant Coronin 1B with a phosphomimetic aspartate substitution at Ser2. Maximal assembly rates were calculated as described in Experimental Procedures.

(C) His-tagged Coronin 1B or Coronin 1B (S2D) was bound to Ni-NTA beads and mixed with 20 nM Arp2/3 complex. Immunoblotting detected Arp2/3 complex bound to the beads.

1B inhibits Arp2/3 complex nucleation in vitro and phosphorylation of Coronin 1B on Ser2 regulates this activity.

Coronin 1B Is Dephosphorylated by an Okadiac Acid-Insensitive Phosphatase

The phosphatase that dephosphorylates and activates Coronin 1B is unknown. To identify this Coronin 1B phosphatase, we developed an assay in which cells were first treated with PMA to stimulate maximal phosphorylation, followed by PMA washout in the presence of a pan-PKC inhibitor (Ro32-0432) to block further phosphorylation. Using this regime, dephosphorylation of Coronin 1B was detected within one minute and phospho-Coronin 1B returned to basal levels by 10 min (Figure 4A). We examined the sensitivity of this phosphatase to the Ser/Thr phosphatase inhibitor okadaic acid, which potently inhibits PP1

(B) Average retrograde flow rates in KD-1B- and NS-expressing cells (three measurements/cell) for each condition are presented as box and whisker plots (dot represents the mean, middle line represents the median, top and bottom of box represent 75% and 25%, respectively, and whiskers represent full data range). Unpaired Student's t test indicates a signification difference between samples ($p < 0.0001$).

(C) KD-1B- and NS-expressing Rat2 cells were subjected to the barbed end assay using Alexa 568-labeled G-actin. Two cells for each condition are shown. Scale bar represents 10 μm.

(D) Quantification of free barbed ends in KD-1B and NS cells. Pixel intensities of Alexa-568-actin around the leading edge were plotted as described in Figure S1. The region encompassing the top 50% of the barbed end signal was defined as the barbed end zone (see Figure S2). Width of this zone in KD-1B and NS cells is presented as a box and whisker plot. Unpaired Student's t test, $p = 0.0165$.

(E) The normalized ratio of barbed ends (Alexa-568 actin) to total actin (Alexa-647 phalloidin) was determined as a function of distance from the cell edge (see Figure S2). Data were from cells shown in (D) and presented as mean ± SEM. Paired Student's t test, $p = 0.013$ for the region 0.3–1.4 μm from the edge.

(F) Platinum replica electron micrographs of lamellipodia in Coronin 1B-depleted and control Rat2 fibroblasts. Expanded view of each cell is presented as an inset. Branched actin filaments are pseudo colored with yellow and green. Scale bar represents 500 nm.

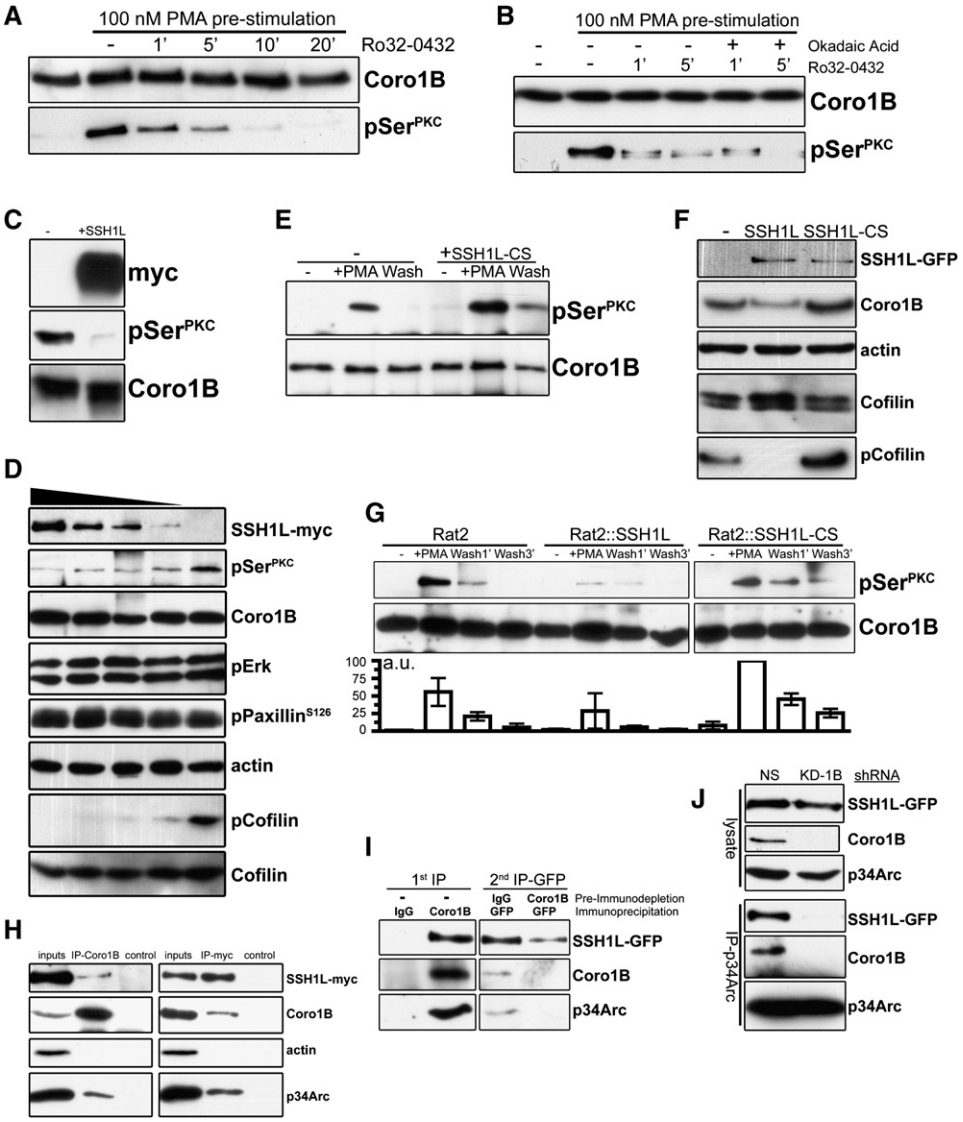

Figure 4. Interactions between Coronin 1B and Slingshot 1L

(A) Rat2 fibroblasts expressing Coronin 1B-GFP were treated with 100 nM PMA to stimulate Coronin 1B phosphorylation. Cells were washed with fresh media and incubated with the pan-PKC inhibitor Ro32-0432 (1 μM) to inhibit further phosphorylation. Coronin 1B was immunoprecipitated from lysates at the indicated times and blotted with anti-pSer^{PKC} to monitor dephosphorylation kinetics.

(B) Dephosphorylation assay carried out as in (A) ± okadiac acid (100 nM).

(C) Recombinant Coronin 1B was phosphorylated in vitro by PKC and subjected to in vitro dephosphorylation with immunoprecipitated SSH1L-myc. Phospho-Coronin 1B was detected with anti-pSer^{PKC}.

(D) Lysates from Rat2 cells that were treated with 100 nM PMA for 30 min were subjected to dephosphorylation in vitro by increasing concentrations of SSH1L-myc. Phospho-Coronin 1B was detected following immunoprecipitation as described above. Phosphorylation of Paxillin^{S126}, Erk1/2 and Cofilin were monitored by immunoblotting the unbound fraction after Coronin 1B immunoprecipitation using phosphospecific antibodies. Blots shown are representative of at least three independent experiments.

(E) Phospho-Coronin 1B was detected in control or HEK293 cells expressing myc-tagged dominant-negative mutant SSH1L C393S (CS) as described in (B).

(F) Lysates of control Rat2 cells or cells expressing either WT SSH1L-GFP or SSH1L-CS-GFP were blotted with the indicated antibodies.

(G) Rat2 cells expressing either WT SSH1L-GFP or CS SSH1L-GFP were subjected to the in vivo dephosphorylation assay. Phospho-Coronin 1B was detected by anti-pSer^{PKC} and quantified by densitometry relative to total Coronin 1B. Results from three independent experiments are presented as means ± SEM.

(H) Lysates from HEK293 cells expressing SSH1L-myc were immunoprecipitated with antibodies to Coronin 1B, SSH1L-myc, or control IgG and blotted with the indicated antibodies.

(I) Endogenous Coronin 1B was immunodepleted from lysates of Rat2 cells expressing SSH1L-GFP. Control rabbit IgG was used for mock depletion. Residual SSH1L-GFP was immunoprecipitated from the immunodepleted lysates using anti-GFP antibody and blotted with the indicated antibodies.

and PP2A (Cohen et al., 1990). Okadaic acid at concentrations from 100 nM (Figure 4B) to 1 μM (data not shown) had no effect on the rate of Coronin 1B dephosphorylation, making it unlikely that phospho-Coronin 1B is a substrate of either PP1 or PP2A.

Coronin 1B Is a Substrate of the Slingshot-1L Phosphatase

We considered whether the Coronin 1B phosphatase might be Slingshot, which acts on Cofilin. Slingshots are among a small number of Ser/Thr phosphatases resistant to okadaic acid (Niwa et al., 2002). To test this hypothesis, we performed in vitro and in vivo dephosphorylation assays using Slingshot-1L (SSH1L). Recombinant Coronin 1B phosphorylated in vitro with purified PKCα was efficiently dephosphorylated by SSH1L (Figure 4C). Since phosphatases often exhibit promiscuous activity on purified proteins, we tested whether SSH1L dephosphorylates Coronin 1B in cell lysates. Coronin 1B was phosphorylated by stimulating cells with PMA prior to lysis and increasing amounts of SSH1L-myc were then added; the phosphorylation status of Coronin 1B and other substrates was monitored by immunoblotting. Coronin 1B was dephosphorylated by SSH1L in a dose-dependent manner (Figure 4D). Cofilin was also efficiently dephosphorylated and may be a preferred substrate. In contrast, no detectable dephosphorylation of phospho-Erk1/2 or phospho-Paxillin was detected, suggesting that the SSH1L phosphatase activity is highly specific under these conditions.

To determine if Coronin 1B is a substrate of SSH1L in vivo, we performed dephosphorylation assays in two different cell types. First, HEK293 cells were transiently transfected with dominant negative mutant form of SSH1L (SSH1L-CS), which harbors a mutation (C393S) in the phosphatase domain that renders it catalytically inactive (Ohta et al., 2003). In the presence of SSH1L-CS, phospho-Coronin 1B was elevated after PMA stimulation and the return to basal levels after washing out PMA was delayed (Figure 4E). Since ectopic SSH1L expression is relatively high in HEK293 cells, we confirmed these observations using Rat2 cells stably expressing lower levels of either wild-type (WT) SSH1L-GFP or dominant negative SSH1L-CS-GFP (Figure 4F). As expected, the level of phosopho-Cofilin decreased in lysates from Rat2 cells expressing WT SSH1L-GFP and increased in lysates from Rat2 cells expressing CS SSH1L-GFP. We conclude that, like Cofilin, Coronin 1B is a substrate of the SSH1L phosphatase in vitro and in vivo.

Coronin 1B, Slingshot 1L, and Arp2/3 Form a Complex In Vivo that Is Bridged by Coronin 1B

Coronin 1B and Arp2/3 complex interact in vivo (Cai et al., 2005). To determine if Slingshot 1L is part of this complex, we immunoprecipitated SSH1L and probed for Coronin 1B and Arp2/3 complex. SSH1L-myc interacted with endogenous Coronin 1B using reciprocal coimmunoprecipitations (Figure 4H). Arp2/3 complex (as reported by the p34 subunit) was detected in both the Coronin 1B and SSH1L immunoprecipitates. Notably, actin was not detected, despite the fact that Coronin 1B, SSH1L and Arp2/3 complex all bind F-actin, indicating that the interaction among these components is not bridged by residual F-actin.

While these results are consistent with the existence of a ternary complex containing Coronin 1B, SSH1L and Arp2/3 complex, they do not exclude the possibility of two bivalent complexes (a Coronin 1B-Arp2/3 complex and a SSH1L-Arp2/3 complex). To identify a ternary complex, we used a two-step immunoprecipitation protocol in which Coronin 1B was first immuno-depleted from the lysates derived from Rat2:SSH1L-GFP cells followed by a second immunoprecipitation of SSH1L-GFP from the depleted lysate (Figure 4I). In the first step, anti-Coronin 1B (but not control IgG) immunoprecipitated both SSH1L-GFP and Arp2/3 complex. When SSH1L-GFP was immunoprecipitated from the Coronin 1B-depleted lysate, no additional Arp2/3 complex was coimmunoprecipitated. In contrast, SSH1L-GFP coimmunoprecipitated both Coronin 1B and Arp2/3 complex from a mock-depleted lysate.

To confirm this result, we tested for an interaction between SSH1L and Arp2/3 complex in Coronin 1B-depleted cells. No SSH1L was detected when Arp2/3 complex was immunoprecipitated from lysates derived from Coronin 1B-depleted, SSH1L-GFP expressing Rat2 (Figure 4J). We conclude that SSH1L, Coronin 1B and Arp2/3 exist in a ternary complex that is bridged by Coronin 1B.

Depletion of Coronin 1B Inhibits SSH1L-Induced Membrane Ruffling

Expression of SSH1L-GFP in Rat2 cells induces constitutive hyper-ruffling at the cell periphery (Figure 5A). Lamellipodia in SSH1L-expressing cells protrude at approximately twice the rate and protrusions are short-lived compared to control cells, with no difference in protrusion distance. Remarkably, depletion of Coronin 1B completely suppressed SSH1L-induced hyper-ruffling. One possible explanation is that Coronin 1B generally influences lamellipodial dynamics by a mechanism unrelated to SSH1L activity. To address this possibility, we investigated lamellipodia in Coronin 1B-depleted cells expressing FP4-CAAX, which induces hyper-ruffling by targeting Ena/VASP proteins to the plasma membrane (Bear et al., 2000, 2002). As expected, expression of FP4-CAAX increased protrusion rate and shortened protrusion persistence, similar to the effects of SSH1L expression, but

(J) Rat2 cells expressing SSH1L-GFP were infected with lentivirus expressing Coronin 1B shRNA (KD-1B) or a control shRNA (NS). Arp2/3 complex was immunoprecipitated using anti-p34Arc and blotted for SSH1L using anti-GFP. Similar results were obtained using anti-GFP to immunoprecitate SSH1L-GFP (data not shown).

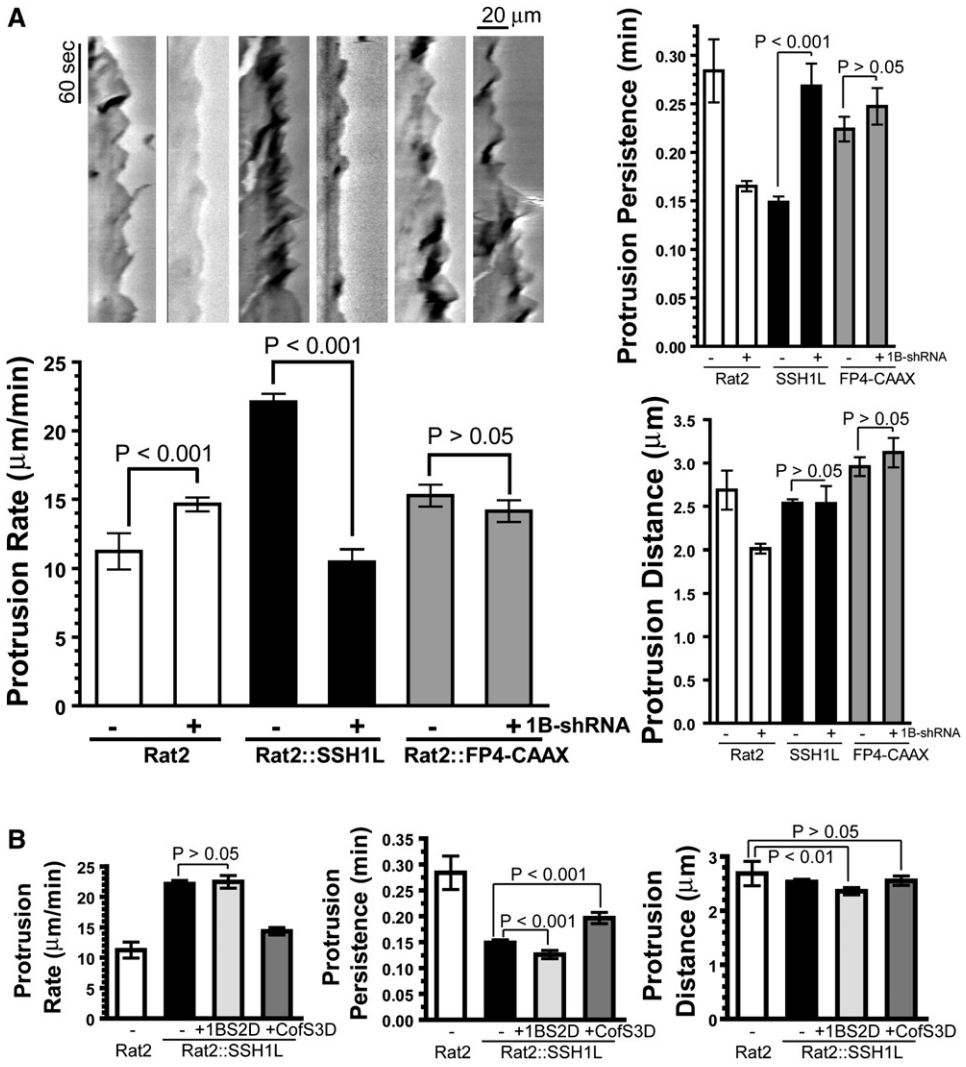

Figure 5. Depletion of Coronin 1B Inhibits SSH1L-Induced Membrane Ruffling

(A) Rat2 cells expressing SSH1L or FP_4-CAAX were transfected with the Coronin 1B shRNA, and subjected to kymography analysis as described in Figure 1E. Newman-Keuls multiple comparison test was used after one-way ANOVA to generate the p values; error bars represent 95% CI.

(B) Phosphomimetic mutants of either Coronin 1B (S2D) or Cofilin (S3D) were coexpressed in Rat2 cells with SSH1L-GFP; kymography analysis was carried out as in Figure 1E; error bars represent 95% CI.

depletion of Coronin 1B had no effect on the ruffling induced by FP4-CAAX. Thus, the suppression of the SSH1L-induced ruffling in Coronin 1B–depleted cells is a specific, rather than a general, effect on lamellipodial dynamics.

Suppression of SSH1L-induced ruffling upon Coronin 1B depletion may occur via dephosphorylation of Coronin 1B by SSH1L. Thus, a phosphomimetic mutant form of Coronin 1B would be predicted to suppress SSH1L-induced hyper-ruffling by competing with endogenous substrates. To test this hypothesis, lamellipodial dynamics were examined in cells expressing Coronin 1B S2D and SSH1L. To our surprise, the Coronin 1B S2D mutant is ineffective in suppressing SSH1L-induced hyper-ruffling (Figure 5B). In contrast, expression of the phosphomimetic Cofilin S3D mutant suppresses SSH1L-induced hyper-ruffling (Figure 5B), confirming that SSH1L-induced ruffling is due to the phosphatase activity of SSH1L. While these results do not preclude a contribution of SSH1L dephosphorylation of Coronin 1B in regulating lamellipodial behavior, they do suggest that regulation of Cofilin by SSH1L influences lamellipodial behavior. Alternately, Cofilin S3D may be a more effective competitor of SSH1L phosphatase than Coronin 1B S2D. Nonetheless, we sought another explanation for the potent suppression of the ectopic SSH1L-induced ruffling upon Coronin 1B depletion.

Depletion of Coronin 1B Disrupts Normal Slingshot 1L Targeting to the Leading Edge

Coronin 1B may act upstream of SSH1L and thereby influence SSH1L-induced hyper-ruffling. For example, Coronin 1B may allow SSH1L to reach its substrate (Cofilin) and thereby influence lamellipodial dynamics. To test this idea, we compared the localization of SSH1L-GFP in control and in Coronin 1B-depleted cells. shRNAs were coexpressed with SSH1L-GFP using a single lentirviral vector (Figure 6A), so that every cell expressing SSH1L-GFP also expressed either Coronin 1B-specific or control shRNA. SSH1L-GFP was not as enriched at the leading edge of Coronin 1B-depleted cells as in the control cells (Figure 6B) when compared to the distribution of Cortactin (see Figure S1). In control shRNA expressing cells, the maximal peaks of Cortactin and SSH1L-GFP were separated by an average of 0.35 μm. In Coronin 1B-depleted cells, Cortactin was distributed identically to that in control cells, but the peak of SSH1L-GFP signal was approximately twice as far rearward from the peak of Cortactin than in control cells (Figure 6C). These data suggest that Coronin 1B is required to target SSH1L to a distinct region within lamellipodia and that proper targeting of SSH1L is required to exert an effect on lamellipodial dynamics.

Previous studies suggested that binding of SSH1L to F-actin targeted it to the leading edge (Nagata-Ohashi et al., 2004). To examine the role of F-actin in localizing SSH1L within lamellipodia, we stained cells expressing SSH1L-GFP (+/− Coronin 1B shRNA) with phalloidin (Figure 6D). In control cells, SSH1L-GFP and F-actin colocalized within lamellipodia, however in Coronin 1B-depleted cells, the distribution of F-actin was indistinguishable from that in control cells at the level of light microscopy, but SSH1L-GFP was excluded from the most distal, F-actin rich region near the leading edge. This result indicates that F-actin is insufficient to target SSH1L to the leading edge, but does not exclude a contribution of F-actin-SSH1L interactions for stimulating phosphatase activity (Nagata-Ohashi et al., 2004; Soosairajah et al., 2005).

Depletion of Coronin 1B Inhibits Endogenous Cofilin Phosphatases

To test whether Coronin 1B depletion also inhibited endogenous Cofilin phosphatase activity, we compared the phospho-Cofilin levels in cells expressing Coronin 1B-shRNA and control shRNA. Cells depleted of Coronin 1B had higher levels of phospho-Cofilin relative to controls (Figure 7A). This effect is not due activation of Cofilin kinases because Coronin 1B-depletion does not alter the level of active LIMK 1/2. To confirm the effect of Coronin 1B depletion on phospho-Cofilin levels, we determined the ratio of active-to-total Cofilin in Coronin 1B-depleted cells using ratiometric imaging (Figure 7B). In control cells, the ratio of active-to-total Cofilin was similar to that in surrounding uninfected cells; in Coronin 1B-depleted cells, the ratio of active-to-total Cofilin is lower than in uninfected cells, particularly in lamellipodial regions (Figure 7B). The ratio of active-to-total Cofilin across the whole cell is approximately 2-fold lower in Coronin 1B-depleted cells (Figure 7C). Together, these results indicate that Coronin 1B enhances dephosphorylation and activation of Cofilin. Moreover, these findings are consistent with the biochemical and cellular effects of ectopic expression of SSH1L-GFP and suggest Coronin 1B influences Cofilin activity via a Slingshot-dependent mechanism.

Activated Cofilin Partially Rescues the Effects of Coronin 1B Depletion on Lamellipodial Dynamics

Since Coronin 1B-depletion increases the amount of phospho-Cofilin, we postulated that the effects on lamellipodial dynamics might be due, in part, to a failure to activate Cofilin at the leading edge. To test this idea, we coexpressed an activated Cofillin mutant (S3A) along with Coronin 1B or control shRNA. Lamellipodial protrusions extended faster and were shorter-lived in cells expressing Cofilin (S3A)-GFP than those in either control cells expressing no Cofilin (S3A)-GFP or non-transfected cells (Figure 7D), similar to the effects of expressing SSH1L-GFP. Coexpression of Cofilin (S3A)-GFP and Coronin 1B shRNA partially suppressed the effects on lamellipodial dynamics of Coronin 1B depletion. Lamellipodial protrusion rate decreased and protrusion persistence was modestly increased, but did not reach control levels. It is important to note that, although Cofilin S3A rescued the lamellipodial dynamics associated with depletion of Coronin 1B, it did not rescue the effects on whole-cell motility (data not shown). Together, these data suggest that Coronin 1B promotes the activation of Cofilin at the leading edge.

DISCUSSION

The Cellular Function of Coronin 1B

Our data indicate that Coronin 1B is a key regulator of whole-cell motility and lamellipodial dynamics. Although Coronin 1B is not absolutely required for cells to move or lamellipodia to protrude, it enhances these processes and is a likely target of signal transduction cascades that regulate motility. Coronin 1B influences motility through control of actin filament dynamics and architecture at the leading edge. In the absence of Coronin 1B, retrograde actin flow is reduced and the dendritic actin meshwork of the lamellipodia is abnormal. These two observations are likely to be aspects of the same underlying phenomenon, as the architecture of the actin network reflects the balance of actin assembly at the front and disassembly at the back of the lamellipodia. Future studies will dissect the relative contributions of actin assembly/disassembly and myosin-based contraction to Coronin 1B's effect on retrograde flow.

Most striking is the different distribution and density of actin barbed ends in the lamellipodia of cells lacking Coronin 1B. Cells depleted of Coronin 1B have higher barbed end density than controls and the barbed ends are concentrated in a narrower zone at the leading edge.

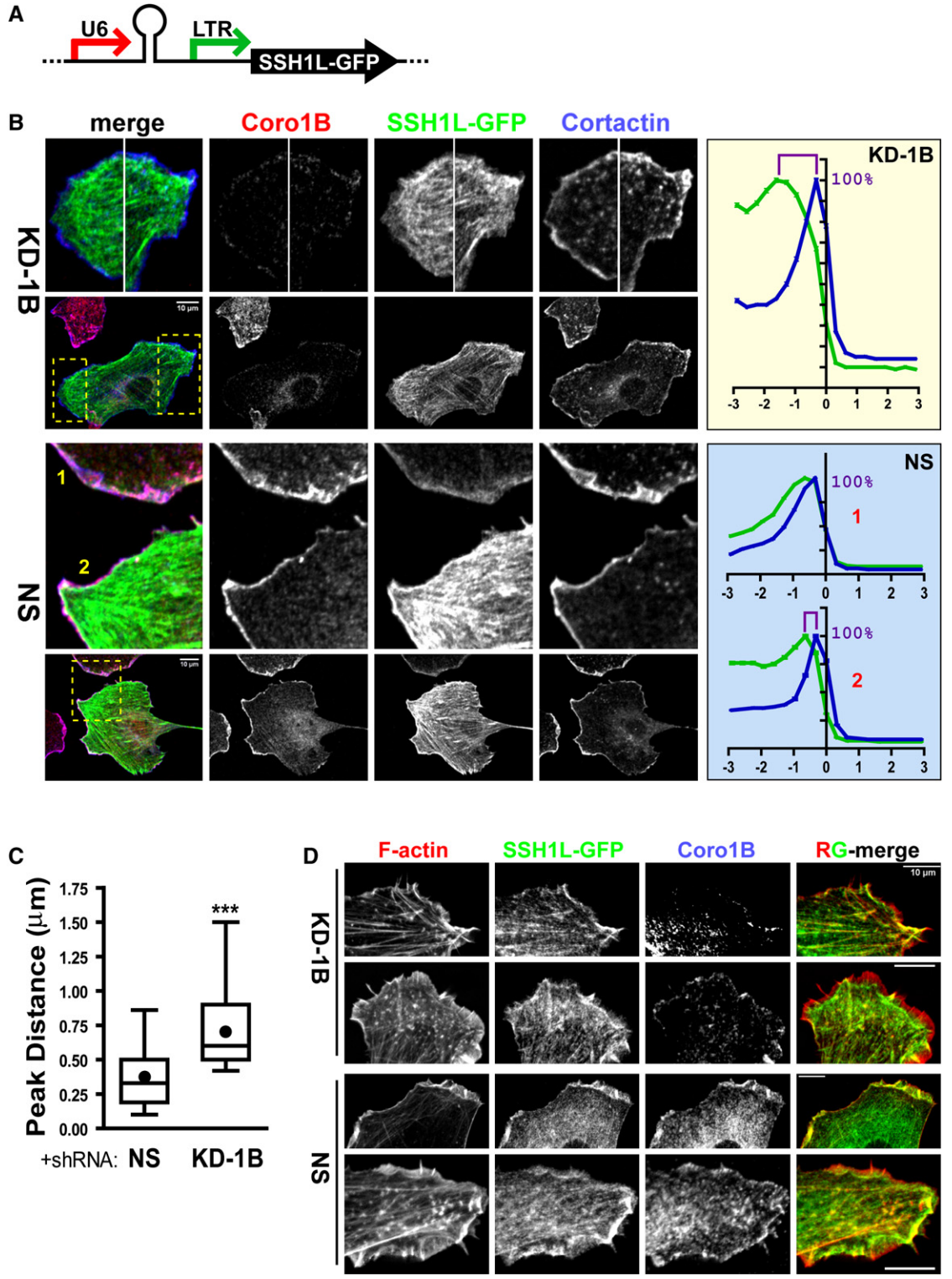

Figure 6. Depletion of Coronin 1B Disrupts Targeting of Slingshot 1L to the Leading Edge

(A) Diagram of the lentiviral vector combining Coronin 1B (KD-1B) or NS control shRNA and SSH1L-GFP expression.

(B) Rat2 cells infected with lentivirus described in (A) were stimulated with EGF and stained for Coronin 1B and Cortactin. Regions boxed by yellow dash lines are magnified in the upper panels. Pixel intensities around the cell edge were extracted and plotted as described in Figure S1. The relative intensities of Cortactin (blue) and SSH1L-GFP (green) are plotted for Coronin 1B-depleted cells (KD-1B, upper panel) and for two control cells (NS, lower panels).

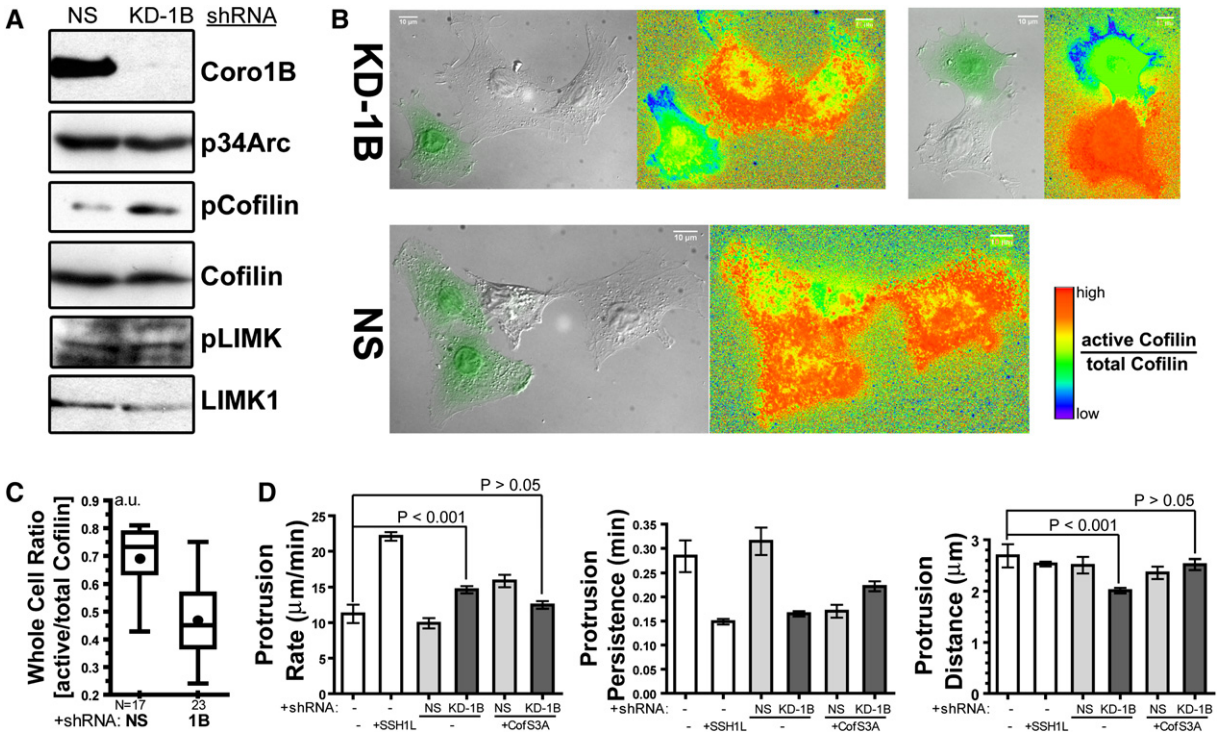

Figure 7. Depletion of Coronin 1B Increases Phosphorylation of Cofilin and Expression of Activated Cofilin (S3A) Partially Rescues the Effects of Coronin 1B Depletion on Lamellipodia Dynamics

(A) Lysates from Rat2 cells expressing either the Coronin 1B shRNA (KD-1B) or control shRNA (NS) were blotted with the indicated antibodies.

(B) Cells generated as described in panel (A) were immunostained for total Cofilin (MAB22) and phospho-Cofilin (4321) and subjected to ratio imaging. GFP-positive cells in the DIC image express either Coronin 1B (KD-1B) or control (NS) shRNA. Ratios of active/total Cofilin were calculated from (total Cofilin – pCofilin) / total Cofilin and presented using a rainbow look-up table.

(C) Active/total Cofilin ratios in whole cells expressing Coronin 1B shRNA (KD-1B) or control shRNA (NS). Whole-cell average ratio from 17 and 23 cells is presented as a box and whisker plot; unpaired Student's t test, $p < 0.0001$.

(D) Rat2 cells expressing activated Cofilin (S3A) and/or Coronin 1B shRNA were subjected to kymography analsysis. Protrusion parameters were determined as described in Figure 1E. ANOVA test shows significant difference between the samples. Newman-Keuls multiple comparison tests were used to generate p values; error bars represent 95% CI.

Increased barbed ends could arise by three mechanisms: failure to cap or uncapping of existing filaments, severing of filaments or de novo nucleation of new filaments. Since Coronin 1B has no detectable capping activity (Figure S6), failure to cap filaments can be eliminated from consideration. The increased barbed ends observed with Coronin 1B depletion are also unlikely to result from increased filament severing since Cofilin is less active in the lamellipodia of knockdown cells. We cannot exclude an effect on Cofilin-independent severing (e.g., Gelsolin), but since Cofilin is required for protrusion, it is probably the predominant severing factor in lamellipodia. We suggest that increased nucleation of filaments most likely results in increased barbed ends in lamellipodia of Coronin 1B-depleted cells.

Coronin 1B Inhibits Arp2/3-Mediated Nucleation in a Phosphoregulated Manner

Consistent with the increased density of barbed ends in lamellipodia of Coronin 1B-depleted cells, recombinant Coronin 1B inhibits the nucleation activity of Arp2/3 in vitro. This inhibitory effect on Arp2/3 activity is a conserved property of Coronins from yeast to humans (Humphries et al., 2002). Other proteins such as Tropomyosin, Caldesmon and EPLIN inhibit Arp2/3 complex nucleation activity, but these proteins are thought to bind tightly to the sides of actin filaments and compete with binding of Arp2/3 complex to the mother actin filament (Blanchoin et al., 2001; Maul et al., 2003; Yamakita et al., 2003) to indirectly inhibit filament-dependent Arp2/3 nucleation activity. In contrast, inhibition by Coronin 1B appears to arise

(C) The distance between the maximal intensity of SSH1L-GFP and that of Cortactin staining was determined for Coronin 1B-depleted or control cells ($n = 27$ cells). Data are presented as a box and whisker plot; unpaired Student's t test, $p < 0.001$.

(D) Cells prepared as described in panel (B) were stained with anti-Coronin 1B and Alexa Fluor 568-phalloidin. RG-merge shows overlap between SSH1L-GFP and F-actin.

from direct binding of Coronin to Arp2/3 complex and stabilization of its ''open'', inactive form (Rodal et al., 2005). Our findings support this notion since Coronin 1B S2D binds poorly to Arp2/3 and has weaker inhibitory activity. Further studies will be required to elucidate the molecular mechanism of Coronin 1B's inhibition of Arp2/3 complex.

Our results suggest that limiting filament nucleation activity via Coronin 1B is important for efficient lamellipodial protrusion. This conclusion is consistent with other studies in which lamellipodial protrusions formed in response to EGF were blocked in cells microinjected with the Arp2/3 complex activating VCA (WA) domain of SCAR or WASP (Shao et al., 2006). Coronin 1B apparently serves to temper filament nucleation by Arp2/3 complex in lamellipodia, especially close to the membrane where several WASP/SCAR coactivating factors, such as Rac, Cdc42 and PIP_2, are enriched. In the absence of Coronin 1B, nucleation by Arp2/3 complex may be overactive, leading to the increased free barbed ends and the faster rate of protrusion observed in Coronin 1B depleted cells. Without a means to limit Arp2/3 complex activity, explosive generation of new filaments could result in short-lived protrusions that stall as G-actin becomes limiting, consistent with the decreased protrusion persistence and distance observed in the Coronin 1B-depleted cells. Previous models for the control of filament nucleation in lamellipodia focused on the localized activation of WASP/SCAR/Formin proteins by inositol lipids and Rho-type GTPases. Our studies suggest that nucleation control is more complex than current models predict and involves a balance between nucleation promoting factors and inhibitors.

Coronin 1B Regulates SSH1L Localization and Cofilin Activity

Coronin 1B is required for SSH-induced lamellipodial activity and for targeting SSH1L within lamellipodia. Through these processes, Coronin 1B could significantly influence the activity of Cofilin at the leading edge. This mechanism for regulating Cofilin activity is analogous to the mechanisms regulating many kinases and phosphatases via targeting subunits and scaffolds (Cohen, 2002; Sim and Scott, 1999). It is important to note that targeting of SSH1L does not override other mechanisms of Slingshot regulation such as phosphorylation or F-actin binding (Nagata-Ohashi et al., 2004). Rather, it is likely that appropriate targeting of SSH1L works in conjunction with these other regulatory events to control Slingshot's activity spatially and temporally.

Our studies in fibroblasts link Coronins and Cofilin activities via SSH, however there is precedence for such a connection in other systems (Goode et al., 1999). Mutations in the single yeast Coronin gene are benign except when combined with mutations in the Cofilin gene. F-actin accumulates in abnormal aggregates in double Coronin/Cofilin mutants, but not with each single mutant, suggesting that these proteins function together to promote actin turnover in this organism. Recent studies also identified Coronin 1A as a factor leading to actin depolymerization in *Listeria* actin tails (Brieher et al., 2006). This study suggested that Coronin 1A-bound F-actin has increased affinity for Cofilin, perhaps due to altered helical twist. One prediction of this idea is that Cofilin may not be recruited to the leading edge in the absence of Coronin. We observed no change in Cofilin distribution at the leading edge in Coronin 1B-depleted cells (Figure S8), but future studies are needed to explicitly test whether Coronin 1B has similar activity to Coronin 1A in this regard. It is possible that Coronins direct Cofilin recruitment and activation via SSH targeting to synergistically control Cofilin activity. Regardless of the precise mechanistic details, a conserved functional connection between Coronins and Cofilin in regulating filament dynamics exists from yeast to humans.

The Coordination of Arp2/3 Complex and Cofilin Activity in Lamellipodia

Why is a factor that coordinates the activities of Arp2/3 complex and Cofilin in lamellipodia necessary? Cell motility is a system-based process that requires precise spatial and temporal control of the individual components. Chemotaxis requires localized and coordinate cytoskeletal remodeling to achieve directional movement toward a chemotactic signal. Our work identifies Coronin 1B as a link between two major components, Cofilin and Arp2/3 complex, that control actin remodeling in many cells. Since factors that coordinate cytoskeletal dynamics are likely to be crucial for directional sensing and motility, Coronin 1B is likely regulated by chemotactic signaling pathways. This idea is supported by the recent observations that thymocytes from Coronin 1A knockout mice are severely defective in chemotaxis toward chemokines (Foger et al., 2006). Future studies will focus on the role that Coronin 1B plays in directed cell motility and on elucidating the molecular mechanism of Coronin 1B action.

EXPERIMENTAL PROCEDURES

Descriptions of plasmid construction, cell culture, and antibodies are in Supplemental Experimental Procedures.

Single Cell Tracking and Kymography Analysis

Migration of Rat2 fibroblasts was analyzed as described with slight modifications (Cai et al., 2005). Cells were infected with lentivirus coexpressing Coronin1B or control shRNA with GFP or hCoronin 1B-GFP. Cells were tracked and whole-cell speed calculated using Tracking Analysis software (Andor Bioimaging). GFP negative cells were analyzed as an internal control. For kymography, 300 images were captured at 1 s intervals and processed using ImageJ. Kymographs were generated from protrusive areas of at least 5 cells per treatment and lamellipodial parameters were calculated as described (Bear et al., 2002). Data were exported to Prism for statistical analysis.

Actin Retrograde Flow Measurement

Rat2 cells were infected with lentivirus that coexpress Coronin 1B or control shRNA and GFP-actin. Images were captured at 1 s intervals using spinning disk confocal microscopy. Kymographs were generated and analyzed as described above.

Analysis of Free Actin Filament Barbed Ends In Vivo

Free actin filament barbed ends were detected in permeabilized fibroblasts as described in Supplemental Experimental Procedures using Alexa568-actin (Bryce et al., 2005). Alexa568-actin incorporation was quantified from the intensity profile around the cell periphery as described for Figure S1. The upper 50% of intensities were used to determine the width of the zone of free barbed ends (Figure S2). The ratio of the barbed end intensity to phalloidin intensity along the edge was normalized and plotted as a function of distance from the cell margin (Figure S2).

Platinum Replica Electron Microscopy

Rat2 cells were infected with lentivirus expressing Coronin 1B or control shRNA for 4 days. Cells were plated onto coverslips coated with 10 μg/ml fibronectin for 4 hr and samples were prepared for platinum replica electron microscopy as described (Svitkina and Borisy, 2005). Images were collected at 6300X using a Philips CM12 microscope at 60 kV using Kodak SO-163 negative film, scanned using an Imacon FlexTight 848 scanner at resolution 2500 dpi and adjusted for publication using Photoshop.

Recombinant Coronin 1B Protein Production

Recombinant Coronin 1B was expressed and purified either from *Drosophila* S2 cells (Invitrogen) or from HEK293 cells as described in Supplemental Experimental Procedures. Phosphorylated Coronin 1B was obtained from HEK293 cells treated for 30 min with 50nM PMA prior to harvesting. The phosphorylation status of Coronin 1B was verified by $pSer^{PKC}$ blotting, immunoprecipitation and by mass spectrometry (Figure S5).

Actin Polymerization Assay

Spectrin F-actin seeds (SAS), actin, pyrene labeled actin, GST-VCA and Arp2/3 complex were prepared as described (Bryan and Coluccio, 1985; DiNubile et al., 1995; Egile et al., 1999; Higgs et al., 1999; Spudich and Watt, 1971). Seeded actin polymerization reactions were performed as described (Barzik et al., 2005) with 1 μM actin (5% pyrene labeled) and 0.2 nM SAS. VCA-induced Arp2/3 nucleation reactions were performed as follows: Coronin 1B and Arp2/3 (20 nM) were mixed in MKEI-50 Buffer and incubated at room temperature for 5 min; reactions were initiated by the simultaneous addition of 1.5 μM actin (5% pyrene labeled, primed with 1 mM EGTA and 0.1 mM $MgCl_2$ for 90 s) and GST-VCA (1 nM or 10 nM). The delay between mixing reactants and recording fluorescence was 20 s. Fluorescence was converted to the molar concentration of F-actin from the fluorescence of completely polymerized (24 hr post reaction) and unpolymerized actin, assuming a critical concentration of 0.1 μM. Maximal actin assembly rates were determined from linear fits of the rate as 0.5-1 μM actin polymer formed during the reactions.

In Vivo Coronin 1B Dephosphorylation Assay

Rat2 cells were treated with 100 nM PMA for 30 min to stimulate Coronin 1B phosphorylation. Cells were then washed with fresh media and incubated in media containing the pan-PKC inhibitor, 1 μM Ro32-4032, for the indicated time. Okadaic acid (up to 1 μM) was included in the washout media in some experiments. Reactions were stopped by lysing the cells in RIPA Buffer and Coronin 1B was immunoprecipitated and blotted with $pSer^{PKC}$ antibody as described (Cai et al., 2005).

In Vitro Slingshot Phosphatase Assay

The in vitro Slingshot phosphatase assay was as described (Nagata-Ohashi et al., 2004; Niwa et al., 2002) with slight modifications; a detailed description is in the Supplemental Experimental Procedures.

Imaging and Lamellipodial Colocalization Analysis

Immunofluorescent staining and imaging were performed as described (Cai et al., 2005). For colocalization analyses, a custom ImageJ macro was used to extract pixel intensity as a function of distance from the leading edge. A detailed explanation of this method is in the Supplemental Experimental Procedures.

Active/Total Cofilin Ratio Imaging

To assess active/total Cofilin ratios, cells were stained with antibodies against Cofilin (MAB22; 1:100) and phospho-Cofilin (4321; 1:170) and processed for immunofluorescence imaging as described in the Supplemental Experimental Procedures. DIC images indicated the outline of the cells. The ImageJ plugin, Ratio Plus (http://rsb.info.nih.gov/ij/plugins/ratio-plus.html) was used to calculate the ratio between phospho-Cofilin and Cofilin staining. The ratio was converted into active/total Cofilin ratio by [(Total Cofilin-phosphoCofilin) / Total Cofilin], normalized and presented using a rainbow look-up table.

Supplemental Data

Supplemental Data include Supplemental Experimental Procedures, Supplemental References, and eight figures and can be found with this article online at http://www.cell.com/cgi/content/full/128/5/915/DC1/.

ACKNOWLEDGMENTS

We are grateful to J. Bamburg (Colorado State University) for providing antibodies to pCofilin (4321) and Cofilin (MAB22) and the protocol to quantify active Cofilin by ratio imaging prior to publication, to A. Makhov and H. Mekeel for help with electron microscopy, to K. Burridge, M. Schaller, F. Gertler, J. Bamburg, and D. Roadcap for critical reading of the manuscript, to E. Izaurralde, M. Wilm, and Y. Durocher for reagents, and to T. Kotova and F. Tariq for technical assistance. Electron microscopy work was supported by National Institutes of Health grant CA-16086 to J.D. Griffith. This work was supported by NIH (GM067222) to D.A.S. and funds from the V Foundation, Melanoma Research Foundation, and Carolina Center for Cancer Nanotechnology Excellence (NCI; 1U54CA119343) to J.E.B.

Received: July 20, 2006
Revised: November 13, 2006
Accepted: January 24, 2007
Published: March 8, 2007

REFERENCES

Agnew, B.J., Minamide, L.S., and Bamburg, J.R. (1995). Reactivation of phosphorylated actin depolymerizing factor and identification of the regulatory site. J. Biol. Chem. *270*, 17582–17587.

Bamburg, J.R. (1999). Proteins of the ADF/cofilin family: essential regulators of actin dynamics. Annu. Rev. Cell Dev. Biol. *15*, 185–230.

Bamburg, J.R., McGough, A., and Ono, S. (1999). Putting a new twist on actin: ADF/cofilins modulate actin dynamics. Trends Cell Biol. *9*, 364–370.

Barzik, M., Kotova, T.I., Higgs, H.N., Hazelwood, L., Hanein, D., Gertler, F.B., and Schafer, D.A. (2005). Ena/VASP proteins enhance actin polymerization in the presence of barbed end capping proteins. J. Biol. Chem. *280*, 28653–28662.

Bear, J.E., Loureiro, J.J., Libova, I., Fassler, R., Wehland, J., and Gertler, F.B. (2000). Negative regulation of fibroblast motility by Ena/VASP proteins. Cell *101*, 717–728.

Bear, J.E., Svitkina, T.M., Krause, M., Schafer, D.A., Loureiro, J.J., Strasser, G.A., Maly, I.V., Chaga, O.Y., Cooper, J.A., Borisy, G.G., and Gertler, F.B. (2002). Antagonism between Ena/VASP Proteins and Actin Filament Capping Regulates Fibroblast Motility. Cell *109*, 509–521.

Blanchoin, L., Pollard, T.D., and Hitchcock-DeGregori, S.E. (2001). Inhibition of the Arp2/3 complex-nucleated actin polymerization and branch formation by tropomyosin. Curr. Biol. *11*, 1300–1304.

Brieher, W.M., Kueh, H.Y., Ballif, B.A., and Mitchison, T.J. (2006). Rapid actin monomer-insensitive depolymerization of Listeria actin comet tails by cofilin, coronin, and Aip1. J. Cell Biol. *175*, 315–324.

Bryan, J., and Coluccio, L.M. (1985). Kinetic analysis of F-actin depolymerization in the presence of platelet gelsolin and gelsolin-actin complexes. J. Cell Biol. *101*, 1236–1244.

Bryce, N.S., Clark, E.S., Leysath, J.L., Currie, J.D., Webb, D.J., and Weaver, A.M. (2005). Cortactin promotes cell motility by enhancing lamellipodial persistence. Curr. Biol. *15*, 1276–1285.

Cai, L., Holoweckyj, N., Schaller, M.D., and Bear, J.E. (2005). Phosphorylation of coronin 1B by protein kinase C regulates interaction with Arp2/3 and cell motility. J. Biol. Chem. *280*, 31913–31923.

Cohen, P., Holmes, C.F., and Tsukitani, Y. (1990). Okadaic acid: a new probe for the study of cellular regulation. Trends Biochem. Sci. *15*, 98–102.

Cohen, P.T. (2002). Protein phosphatase 1–targeted in many directions. J. Cell Sci. *115*, 241–256.

Condeelis, J., Hall, A., Bresnick, A., Warren, V., Hock, R., Bennett, H., and Ogihara, S. (1988). Actin polymerization and pseudopod extension during amoeboid chemotaxis. Cell Motil. Cytoskeleton *10*, 77–90.

Dawe, H.R., Minamide, L.S., Bamburg, J.R., and Cramer, L.P. (2003). ADF/cofilin controls cell polarity during fibroblast migration. Curr. Biol. *13*, 252–257.

de Hostos, E.L., Rehfuess, C., Bradtke, B., Waddell, D.R., Albrecht, R., Murphy, J., and Gerisch, G. (1993). Dictyostelium mutants lacking the cytoskeletal protein coronin are defective in cytokinesis and cell motility. J. Cell Biol. *120*, 163–173.

DesMarais, V., Ghosh, M., Eddy, R., and Condeelis, J. (2005). Cofilin takes the lead. J. Cell Sci. *118*, 19–26.

DesMarais, V., Macaluso, F., Condeelis, J., and Bailly, M. (2004). Synergistic interaction between the Arp2/3 complex and cofilin drives stimulated lamellipod extension. J. Cell Sci. *117*, 3499–3510.

DiNubile, M.J., Cassimeris, L., Joyce, M., and Zigmond, S.H. (1995). Actin filament barbed-end capping activity in neutrophil lysates: the role of capping protein-beta 2. Mol. Biol. Cell *6*, 1659–1671.

Egile, C., Loisel, T.P., Laurent, V., Li, R., Pantaloni, D., Sansonetti, P.J., and Carlier, M.F. (1999). Activation of the CDC42 effector N-WASP by the Shigella flexneri IcsA protein promotes actin nucleation by Arp2/3 complex and bacterial actin- based motility. J. Cell Biol. *146*, 1319–1332.

Foger, N., Rangell, L., Danilenko, D.M., and Chan, A.C. (2006). Requirement for coronin 1 in T lymphocyte trafficking and cellular homeostasis. Science *313*, 839–842.

Gohla, A., Birkenfeld, J., and Bokoch, G.M. (2005). Chronophin, a novel HAD-type serine protein phosphatase, regulates cofilin-dependent actin dynamics. Nat. Cell Biol. *7*, 21–29.

Goode, B.L., Wong, J.J., Butty, A.C., Peter, M., McCormack, A.L., Yates, J.R., Drubin, D.G., and Barnes, G. (1999). Coronin promotes the rapid assembly and cross-linking of actin filaments and may link the actin and microtubule cytoskeletons in yeast. J. Cell Biol. *144*, 83–98.

Higgs, H.N., Blanchoin, L., and Pollard, T.D. (1999). Influence of the C terminus of Wiskott-Aldrich syndrome protein (WASp) and the Arp2/3 complex on actin polymerization. Biochemistry *38*, 15212–15222.

Hinz, B., Alt, W., Johnen, C., Herzog, V., and Kaiser, H.W. (1999). Quantifying lamella dynamics of cultured cells by SACED, a new computer- assisted motion analysis. Exp. Cell Res. *251*, 234–243.

Hotulainen, P., Paunola, E., Vartiainen, M.K., and Lappalainen, P. (2005). Actin-depolymerizing factor and cofilin-1 play overlapping roles in promoting rapid F-actin depolymerization in mammalian nonmuscle cells. Mol. Biol. Cell *16*, 649–664.

Huang, T.Y., Dermardirossian, C., and Bokoch, G.M. (2006). Cofilin phosphatases and regulation of actin dynamics. Curr. Opin. Cell Biol. *18*, 26–31.

Humphries, C.L., Balcer, H.I., D'Agostino, J.L., Winsor, B., Drubin, D.G., Barnes, G., Andrews, B.J., and Goode, B.L. (2002). Direct regulation of Arp2/3 complex activity and function by the actin binding protein coronin. J. Cell Biol. *159*, 993–1004.

Ichetovkin, I., Grant, W., and Condeelis, J. (2002). Cofilin produces newly polymerized actin filaments that are preferred for dendritic nucleation by the Arp2/3 complex. Curr. Biol. *12*, 79–84.

Maul, R.S., Song, Y., Amann, K.J., Gerbin, S.C., Pollard, T.D., and Chang, D.D. (2003). EPLIN regulates actin dynamics by cross-linking and stabilizing filaments. J. Cell Biol. *160*, 399–407.

Mishima, M., and Nishida, E. (1999). Coronin localizes to leading edges and is involved in cell spreading and lamellipodium extension in vertebrate cells. J. Cell Sci. *112*, 2833–2842.

Nagata-Ohashi, K., Ohta, Y., Goto, K., Chiba, S., Mori, R., Nishita, M., Ohashi, K., Kousaka, K., Iwamatsu, A., Niwa, R., et al. (2004). A pathway of neuregulin-induced activation of cofilin-phosphatase Slingshot and cofilin in lamellipodia. J. Cell Biol. *165*, 465–471.

Nishita, M., Tomizawa, C., Yamamoto, M., Horita, Y., Ohashi, K., and Mizuno, K. (2005). Spatial and temporal regulation of cofilin activity by LIM kinase and Slingshot is critical for directional cell migration. J. Cell Biol. *171*, 349–359.

Niwa, R., Nagata-Ohashi, K., Takeichi, M., Mizuno, K., and Uemura, T. (2002). Control of actin reorganization by Slingshot, a family of phosphatases that dephosphorylate ADF/cofilin. Cell *108*, 233–246.

Ohta, Y., Kousaka, K., Nagata-Ohashi, K., Ohashi, K., Muramoto, A., Shima, Y., Niwa, R., Uemura, T., and Mizuno, K. (2003). Differential activities, subcellular distribution and tissue expression patterns of three members of Slingshot family phosphatases that dephosphorylate cofilin. Genes Cells *8*, 811–824.

Ponti, A., Matov, A., Adams, M., Gupton, S., Waterman-Storer, C.M., and Danuser, G. (2005). Periodic patterns of actin turnover in lamellipodia and lamellae of migrating epithelial cells analyzed by quantitative Fluorescent Speckle Microscopy. Biophys. J. *89*, 3456–3469.

Rodal, A.A., Sokolova, O., Robins, D.B., Daugherty, K.M., Hippenmeyer, S., Riezman, H., Grigorieff, N., and Goode, B.L. (2005). Conformational changes in the Arp2/3 complex leading to actin nucleation. Nat. Struct. Mol. Biol. *12*, 26–31.

Rubinson, D.A., Dillon, C.P., Kwiatkowski, A.V., Sievers, C., Yang, L., Kopinja, J., Rooney, D.L., Ihrig, M.M., McManus, M.T., Gertler, F.B., et al. (2003). A lentivirus-based system to functionally silence genes in primary mammalian cells, stem cells and transgenic mice by RNA interference. Nat. Genet. *33*, 401–406.

Shao, D., Forge, A., Munro, P.M., and Bailly, M. (2006). Arp2/3 complex-mediated actin polymerisation occurs on specific pre-existing networks in cells and requires spatial restriction to sustain functional lamellipod extension. Cell Motil. Cytoskeleton *63*, 395–414.

Sim, A.T., and Scott, J.D. (1999). Targeting of PKA, PKC and protein phosphatases to cellular microdomains. Cell Calcium *26*, 209–217.

Soosairajah, J., Maiti, S., Wiggan, O., Sarmiere, P., Moussi, N., Sarcevic, B., Sampath, R., Bamburg, J.R., and Bernard, O. (2005). Interplay between components of a novel LIM kinase-slingshot phosphatase complex regulates cofilin. EMBO J. *24*, 473–486.

Spudich, J.A., and Watt, S. (1971). The regulation of rabbit skeletal muscle contraction. I. Biochemical studies of the interaction of the tropomyosin-troponin complex with actin and the proteolytic fragments of myosin. J. Biol. Chem. *246*, 4866–4871.

Stanyon, C.A., and Bernard, O. (1999). LIM-kinase1. Int. J. Biochem. Cell Biol. *31*, 389–394.

Svitkina, T.M., and Borisy, G.G. (1999). Arp2/3 complex and actin depolymerizing factor/cofilin in dendritic organization and treadmilling of actin filament array in lamellipodia. J. Cell Biol. *145*, 1009–1026.

Svitkina, T.M., and Borisy, G.G. (2005). Correlative light and electron microscopy studies of cytoskeletal dynamics. Cell Biology: A Laboratory Handbook, Third Edition, J. Celis, ed. *3*, 277–286.

Symons, M.H., and Mitchison, T.J. (1991). Control of actin polymerization in live and permeabilized fibroblasts. J. Cell Biol. *114*, 503–513.

Uetrecht, A.C., and Bear, J.E. (2006). Coronins: the return of the crown. Trends Cell Biol. *16*, 421–426.

Yamakita, Y., Oosawa, F., Yamashiro, S., and Matsumura, F. (2003). Caldesmon inhibits Arp2/3-mediated actin nucleation. J. Biol. Chem. *278*, 17937–17944.

Zhou, Q., Homma, K.J., and Poo, M.M. (2004). Shrinkage of dendritic spines associated with long-term depression of hippocampal synapses. Neuron *44*, 749–757.